

PG 1553+113: FIVE YEARS OF OBSERVATIONS WITH MAGIC

J. ALEKSIĆ¹, L. A. ANTONELLI², P. ANTORANZ³, M. BACKES⁴, J. A. BARRIO⁵, D. BASTIERI⁶, J. BECERRA GONZÁLEZ^{7,8},
W. BEDNAREK⁹, A. BERDYUGIN¹⁰, K. BERGER^{7,8}, E. BERNARDINI¹¹, A. BILAND¹², O. BLANCH¹, R. K. BOCK¹³,
A. BOLLER¹², G. BONNOLI², D. BORLA TRIDON¹³, I. BRAUN¹², T. BRETZ^{14,26}, A. CANELLAS¹⁵, E. CARMONA¹³,
A. CAROSI², P. COLIN¹³, E. COLOMBO⁷, J. L. CONTRERAS⁵, J. CORTINA¹, L. COSSIO¹⁶, S. COVINO², F. DAZZI^{16,27}, A. DE
ANGELIS¹⁶, E. DE CEA DEL POZO¹⁷, B. DE LOTTO¹⁶, C. DELGADO MENDEZ^{7,28}, A. DIAGO ORTEGA^{7,8}, M. DOERT⁴,
A. DOMÍNGUEZ¹⁸, D. DOMINIS PRESTER¹⁹, D. DORNER¹², M. DORO²⁰, D. ELSAESSER¹⁴, D. FERENC¹⁹, M. V. FONSECA⁵,
L. FONT²⁰, C. FRUCK¹³, R. J. GARCÍA LÓPEZ^{7,8}, M. GARCZARCZYK⁷, D. GARRIDO²⁰, G. GIAVITTO¹, N. GODINOVIĆ¹⁹,
D. HADASCH¹⁷, D. HÄFNER¹³, A. HERRERO^{7,8}, D. HILDEBRAND¹², J. HOSE¹³, D. HRUPEC¹⁹, B. HUBER¹², T. JOGLER¹³,
S. KLEPSE¹, T. KRÄHENBÜHL¹², J. KRAUSE¹³, A. LA BARBERA², D. LELAS¹⁹, E. LEONARDO³, E. LINDFORS¹⁰,
S. LOMBARDI⁶, M. LÓPEZ⁵, E. LORENZ^{12,13}, M. MAKARIEV²¹, G. MANEVA²¹, N. MANKUZHIIYIL¹⁶, K. MANNHEIM¹⁴,
L. MARASCHI², M. MARIOTTI⁶, M. MARTÍNEZ¹, D. MAZIN^{1,13}, M. MEUCCI³, J. M. MIRANDA³, R. MIRZOYAN¹³,
H. MIYAMOTO¹³, J. MOLDÓN¹⁵, A. MORALEJO¹, D. NIETO⁵, K. NILSSON^{10,29}, R. ORITO¹³, I. OYA⁵, R. PAOLETTI³,
S. PARDO⁵, J. M. PAREDES¹⁵, S. PARTINI³, M. PASANEN¹⁰, F. PAUSS¹², M. A. PEREZ-TORRES¹, M. PERSIC^{16,22},
L. PERUZZO⁶, M. PILIA²³, J. POCHON⁷, F. PRADA¹⁸, P. G. PRADA MORONI²⁴, E. PRANDINI^{6,*}, I. PULJAK¹⁹,
I. REICHARDT¹, R. REINTHAL¹⁰, W. RHODE⁴, M. RIBÓ¹⁵, J. RICO^{25,1}, S. RÜGAMER¹⁴, A. SAGGION⁶, K. SAITO¹³,
T. Y. SAITO¹³, M. SALVATI², K. SATALECKA¹¹, V. SCALZOTTO⁶, V. SCAPIN⁵, C. SCHULTZ⁶, T. SCHWEIZER¹³,
M. SHAYDUK¹³, S. N. SHORE²⁴, A. SILLANPÄÄ¹⁰, J. SITAREK⁹, D. SOB CZYNSKA⁹, F. SPANIER¹⁴, S. SPIRO², A. STAMERRA³,
B. STEINKE¹³, J. STORZ¹⁴, N. STRAH⁴, T. SURIĆ¹⁹, L. TAKALO¹⁰, F. TAVECCHIO^{2,*}, P. TEMNIKOV²¹, T. TERZIĆ¹⁹,
D. TESCARO¹, M. TESHIMA¹³, M. THOM⁴, O. TIBOLLA¹⁴, D. F. TORRES^{25,17}, A. TREVES²³, H. VANKOV²¹, P. VOGLER¹²,
R. M. WAGNER¹³, Q. WEITZEL¹², V. ZABALZA¹⁵, F. ZANDANEL¹⁸, R. ZANIN¹,

¹ IFAE, Edifici Cn., Campus UAB, E-08193 Bellaterra, Spain

² INAF National Institute for Astrophysics, I-00136 Rome, Italy

³ Università di Siena, and INFN Pisa, I-53100 Siena, Italy

⁴ Technische Universität Dortmund, D-44221 Dortmund, Germany

⁵ Universidad Complutense, E-28040 Madrid, Spain

⁶ Università di Padova and INFN, I-35131 Padova, Italy

⁷ Inst. de Astrofísica de Canarias, E-38200 La Laguna, Tenerife, Spain

⁸ Depto. de Astrofísica, Universidad de La Laguna, E-38206 La Laguna, Spain

⁹ University of Łódź, PL-90236 Lodz, Poland

¹⁰ Tuorla Observatory, University of Turku, FI-21500 Piikkiö, Finland

¹¹ Deutsches Elektronen-Synchrotron (DESY), D-15738 Zeuthen, Germany

¹² ETH Zurich, CH-8093 Switzerland

¹³ Max-Planck-Institut für Physik, D-80805 München, Germany

¹⁴ Universität Würzburg, D-97074 Würzburg, Germany

¹⁵ Universitat de Barcelona (ICC/IEEC), E-08028 Barcelona, Spain

¹⁶ Università di Udine, and INFN Trieste, I-33100 Udine, Italy

¹⁷ Institut de Ciències de l'Espai (IEEC-CSIC), E-08193 Bellaterra, Spain

¹⁸ Inst. de Astrofísica de Andalucía (CSIC), E-18080 Granada, Spain

¹⁹ Croatian MAGIC Consortium, Institute R. Boskovic, University of Rijeka and University of Split, HR-10000 Zagreb, Croatia

²⁰ Universitat Autònoma de Barcelona, E-08193 Bellaterra, Spain

²¹ Inst. for Nucl. Research and Nucl. Energy, BG-1784 Sofia, Bulgaria

²² INAF/Osservatorio Astronomico and INFN, I-34143 Trieste, Italy

²³ Università dell'Insubria, Como, I-22100 Como, Italy

²⁴ Università di Pisa, and INFN Pisa, I-56126 Pisa, Italy

²⁵ ICREA, E-08010 Barcelona, Spain

²⁶ now at: Ecole polytechnique fédérale de Lausanne (EPFL), Lausanne, Switzerland

²⁷ supported by INFN Padova

²⁸ now at: Centro de Investigaciones Energéticas, Medioambientales y Tecnológicas (CIEMAT), Madrid, Spain

²⁹ now at: Finnish Centre for Astronomy with ESO (FINCA), Turku, Finland

and

* corresponding authors. E-mail: elisa.prandini@pd.infn.it, fabrizio.tavecchio@brera.inaf.it

Draft version June 2, 2019

ABSTRACT

We present the results of five years (2005–2009) of MAGIC observations of the BL Lac object PG 1553+113 at very high energies (VHEs). Adding the new data set (2007–2009) to previous observations, this source becomes one of the best long-term followed sources at energies above 100 GeV. Power law fits of the individual years are compatible with a steady mean photon index $\Gamma = 4.27 \pm 0.14$. In the last three years of data, the flux level above 150 GeV shows a marginal variability, in the range from 4% to 11% of the Crab Nebula flux. Simultaneous optical data also show only modest variability that seems to be correlated with VHE gamma-ray variability. We also performed a temporal analysis of all available *Fermi*/LAT data of PG 1553+113 above 1 GeV, which reveals a clear variability in the 2008–2009 sample. Finally, we present a combination of the mean spectrum measured at very high energies with archival data available for other wavelengths. The mean spectral energy distribution can be modeled with a one-zone SSC model, which gives the main physical parameters governing the

VHE emission in the blazar jet.

Subject headings: radiation mechanisms: non-thermal, gamma-rays: observations, BL Lacertae objects: individual (PG 1553+113)

1. INTRODUCTION

The majority of extragalactic γ -ray sources, both at GeV energies and above 100 GeV, are blazars, radio-loud active galactic nuclei with a relativistic jet pointing towards the Earth. Their emission is dominated by the non-thermal continuum produced within the jet and boosted by relativistic effects (Urry & Padovani 1995). The spectral energy distribution (SED) displays two broad peaks, widely interpreted as due to synchrotron, low frequency peak, and inverse Compton, high frequency peak, mechanism (although the high energy peak could also be the result of hadronic processes, as proposed in Mannheim 1993). Among blazars, BL Lac objects are characterized by extremely weak emission lines in their optical spectra, which often makes a measurement of their redshift difficult. The large majority of extragalactic sources detected above 100 GeV are BL Lac objects, in which the peak of the synchrotron bump is located in the UV-X-ray bands and the high energy peak around 100 GeV (these sources are often called high frequency peaked BL Lacs, HBLs). PG 1553+113 is a BL Lac discovered by Green et al. (1986). The large X-ray to radio flux ratio makes this source a typical HBL. Indeed, its synchrotron peak is located between the UV and X-ray bands. Its optical spectrum is featureless, preventing the direct determination of the redshift. Indirect methods based on the non detection of the host galaxy provide lower limits, ranging from 0.09 to 0.78 (Sbarufatti, Treves, & Falomo 2005; Treves et al. 2007). The most recent estimate, based on the Ly alpha forest method, gives 0.40–0.45 (Danforth et al. 2010).

PG 1553+113 has been discovered as a VHE γ -ray emitter by H.E.S.S. (Aharonian et al. 2006a) and MAGIC (Albert et al. 2007a), with a flux of approximately 2% of that of the Crab Nebula above 200 GeV. The spectrum appears extremely soft (photon index $\Gamma \sim 4$), as expected by the absorption of VHE photons through interaction with the Extragalactic Background Light (EBL) if the source is located at relatively large redshift (Stecker de Jager & Salamon 1992).

VHE γ -ray observations have been used as alternative method to constrain the distance of blazars. Aharonian et al. (2006b) proposed a way to set an upper limit on the distance of blazars based on the assumption that the VHE intrinsic spectrum, obtained by correcting the observed spectrum for the extragalactic background light absorption, cannot be harder than a fixed value given by theory. The technique, applied to PG 1553+113, lead to an upper limit of $z < 0.74$. Recently, Prandini et al. (2010) extended this method using the spectrum measured at lower energies as limiting slope for the original spectrum, obtaining $z < 0.66$ for PG 1553+113, at 2σ level. Other approaches require the absence of a pile up at high energies. With this method, Mazin & Goebel (2007) get $z < 0.42$. Hence, in the case of PG 1553+113, the upper limits obtained with these methods are in the range of the limits set by optical measurements. In this work we adopt the redshift

$z = 0.40$. Such a large redshift is also supported by the absence of significant points at energies above 700 GeV in the spectrum of the source.

At MeV-GeV energies, PG 1553+113 was not detected by EGRET, but it is well visible by the Large Area Telescope (LAT) on-board *Fermi*, being detected with a significance above 10σ already in the first three months of observations (Abdo et al. 2009a). Abdo et al. (2010b) show that the *Fermi*/LAT spectrum is surprisingly constant both in normalization and slope over ~ 200 days. Interestingly, a stability of the spectrum was also suggested by the H.E.S.S. and MAGIC observations, showing rather marginal variability during 2005 and 2006 observations. The stability of the VHE γ -ray emission is in contrast to the behavior commonly observed in other TeV emitting BL Lacs, showing rather pronounced variations at all timescales.

After its discovery, PG 1553+113 was regularly observed by MAGIC. In this paper, we present the analysis of the new data taken from 2007 to 2009, combined with previous observations. The differential and integral fluxes are analyzed, in comparison with partially simultaneous measurements at other wavelengths, and the stability of the spectrum over this long period is studied. Finally, we combine all the data available and model the SED with a one-zone Synchrotron Self Compton (SSC) model, constraining the main physical parameters that govern the VHE emission in the blazar jet.

2. MAGIC OBSERVATIONS AND DATA ANALYSIS

Since autumn 2009, MAGIC (Cortina et al. 2009) is a stereo system composed by two Imaging Atmospheric Cherenkov Telescopes (IACTs) located on La Palma, Canary Islands, Spain (28.75°N, 17.89°W, 2240 m asl). In this paper, we present only data collected before the stereo upgrade, with a single telescope, MAGIC I (Baixeras et al. 2004), hereafter called MAGIC. The parabolic-shaped reflector, with a total mirror area of 236 m², allows MAGIC to collect the Cherenkov light and focus it onto a multi-pixel camera, composed of 577 photo-multipliers. MAGIC camera and trigger are designed to record data also under moderate light conditions (i.e. moderate moon, twilight). Due to its comparatively low trigger energy threshold of ~ 50 GeV, MAGIC is well suited to perform multiwavelength observations together with instruments operating in the GeV range.

The total field of view of the MAGIC camera is 3.5°, and the effective collection area is of the order of 10⁵ m² at 200 GeV for a source close to zenith. The incident light pulses are converted into analog signals, transmitted via optical fibers and digitised by 2 GHz fast analog to digital converters (FADCs).

PG 1553+113 was observed with the MAGIC telescope for nearly 19 hours in 2005 and 2006 (Albert et al. 2007a); it was also the subject of a multiwavelength campaign carried out in July 2006 with optical, X-ray and TeV γ -ray telescopes (Albert et al. 2009). Here, we present the results of follow-up observations, performed for 14 hours in March-April 2007, for nearly 26 hours

TABLE 1
PG 1553+113 FINAL DATA SET

Cycle	Date	Eff. Time [min]	Zd [°]	Rate [Hz]	DC [μ A]
III	23/03/2007	58	19 - 29	164	dark night
	19/04/2007	32	22 - 28	155	dark night
	20/04/2007	150	17 - 29	163	dark night
	21/04/2007	115	17 - 24	155	dark night
	22/04/2007	101	17 - 23	162	dark night
	23/04/2007	143	17 - 27	161	dark night
	24/04/2007	92	17 - 23	160	dark night
IV	17/03/2008	58	17 - 19	150	dark night
	18/03/2008	26	18 - 19	150	dark night
	01/04/2008	43	20 - 26	167	dark night
	05/04/2008	109	17 - 31	167	dark night
	13/04/2008	97	17 - 22	147	dark night
	29/04/2008	44	27 - 36	151	dark night
	03/05/2008	24	26 - 31	146	dark night
	04/05/2008	40	28 - 36	155	dark night
	05/05/2008	38	26 - 33	150	dark night
	07/05/2008	40	28 - 36	153	dark night
V	16/04/2009	93	17 - 27	133	2.8 - 3.7
	17/04/2009	103	17 - 28	151	1.6 - 2.4
	18/04/2009	126	17 - 28	168	0.7 - 1.7
	20/04/2009	73	19 - 35	171	0.9 - 1.4
	21/04/2009	57	23 - 34	177	0.8 - 1.0
	15/06/2009	57	24 - 35	125	0.8 - 2.1

^aPG 1553+113 data set from 2007 to 2009 used in this study. From left to right: MAGIC Cycle of observation, first column, and corresponding dates in dd/mm/yy, second column; effective time of observation in minutes and zenith angle range in degrees, third and fourth column. In the last two columns, the rate of the events after the image cleaning, in Hz, and the mean DC current in the camera, in unit of μ A, are shown. The night is considered as dark night, if the DC current while observing an extragalactic object is less than indicatively 1.2 μ A.

in March-May 2008, some of those simultaneously with other instruments (Aleksić et al. 2010), and for about 24 hours in March-July 2009, which were partly taken in moderate light conditions (moon light). Unfortunately, both 2008 and 2009 observations were severely affected by bad weather (including *calima*, i.e. Saharan sand-dust in the atmosphere) that reduced the final data set and resulted in an increased energy threshold.

All data analyzed here were taken in the false-source tracking (wobble) mode (Fomin et al. 1994), in which the telescope pointing was alternated every 20 minutes between two sky positions at 0.4° offset from the source. The zenith angle of 2007 observations varied from 17° to 30° , in 2008 it extended up to 36° , while in 2009 it covered the range from 17° to 35° .

The data were analyzed using the standard MAGIC analysis chain (Albert et al. 2008a; Aliu et al. 2009). Severe quality cuts based on event rate after night sky background suppression were applied to the sample; 28.7 hours of good quality data remained after these cuts, out of which 11.5 hours were taken in 2007, 8.7 hours in 2008 and 8.5 hours in 2009. More details about the final data set can be found in Table 1. For the signal study, a cut in the parameter *size* removed events with a total charge less than 80 photo-electrons (phe) in the 2007 data set, and 200 phe in 2008 and 2009 data sets. In the latter case, this cut reduces the effect of the moon light.

Finally, for the spectrum determination an additional cut in PMT DC current, namely above 2.5 μ A, was ap-

TABLE 2
PG 1553+113 SIGNAL

Year	Time [h]	Opt. PSF [mm]	Energy Th. [GeV]	Excesses	Signif. [σ]
2007	11.5	13	80	1400 ± 242	5.8
2008	8.7	13	150	542 ± 69	8.1
2009	8.5	14.8	160	212 ± 52	4.2

^aPG 1553+113 signal study. From left to right: year of observation, effective time of good quality data used for the signal analysis, optical point spread function (PSF), energy threshold of the analysis, number of excess events observed and significance of the signal.

plied to the 2009 sample, in order to reduce systematics due to the moon light (Britzger et al. 2009), resulting in 6.9 hours of good quality data. For the conclusive steps of the analysis, Monte-Carlo (MC) simulations of γ -like events were used. Hadronic background suppression was achieved using the Random Forest (RF) method (Albert et al. 2008c), in which each event is assigned an additional parameter, the *hadronness*, which is related to the probability that the event is not γ -like. The RF method was also used in the energy estimation. The threshold of the analysis was estimated to be 80 GeV in 2007, 150 GeV in 2008 and 160 GeV in 2009, as shown in Table 2.

Due to changes in the telescope performance, the *sigma* of the optical point-spread function (PSF) of 2007 and 2008 was measured to be 13.0 mm, while in 2009 it was 14.9 mm. To take all these differences into account, the data were analysed separately, using dedicated sets of simulated data. Effects on the spectrum determination introduced by the limited energy resolution were corrected by unfolding the final spectra (Albert et al. 2007b).

3. VHE γ -RAY RESULTS

The 28.7 hours of good quality observations of PG 1553+113 carried out between 2007 and 2009 resulted in a signal of 8.8σ of significance according to eq. 17 of Li & Ma (1983), obtained by combining the results from each year, listed in Table 2. The signal was extracted by analyzing the distribution of the parameter *alpha*, related to the incoming direction of the primary cosmic ray inducing the atmospheric shower. Images induced by primary gammas have this parameter close to zero because of their preferential direction, while images due to hadrons have a random distribution of *alpha* (the direction of hadrons is nearly isotropic). More details on the signal extraction with the *alpha* technique can be found in Albert et al. 2008b. For the signal detection, no cut in energy was applied.

The significance of the signal was 5.8σ in 2007, 8.1σ in 2008 and 4.2σ in 2009. Hence, the source was detected by MAGIC every year, indicating that PG 1553+113 is a stable presence in the VHE sky. Due to a large difference in the energy thresholds and changes in the experimental conditions, we cannot extract any further information from the obtained integral significance; a detailed spectral analysis is necessary in order to study the source emission.

3.1. Integral Flux

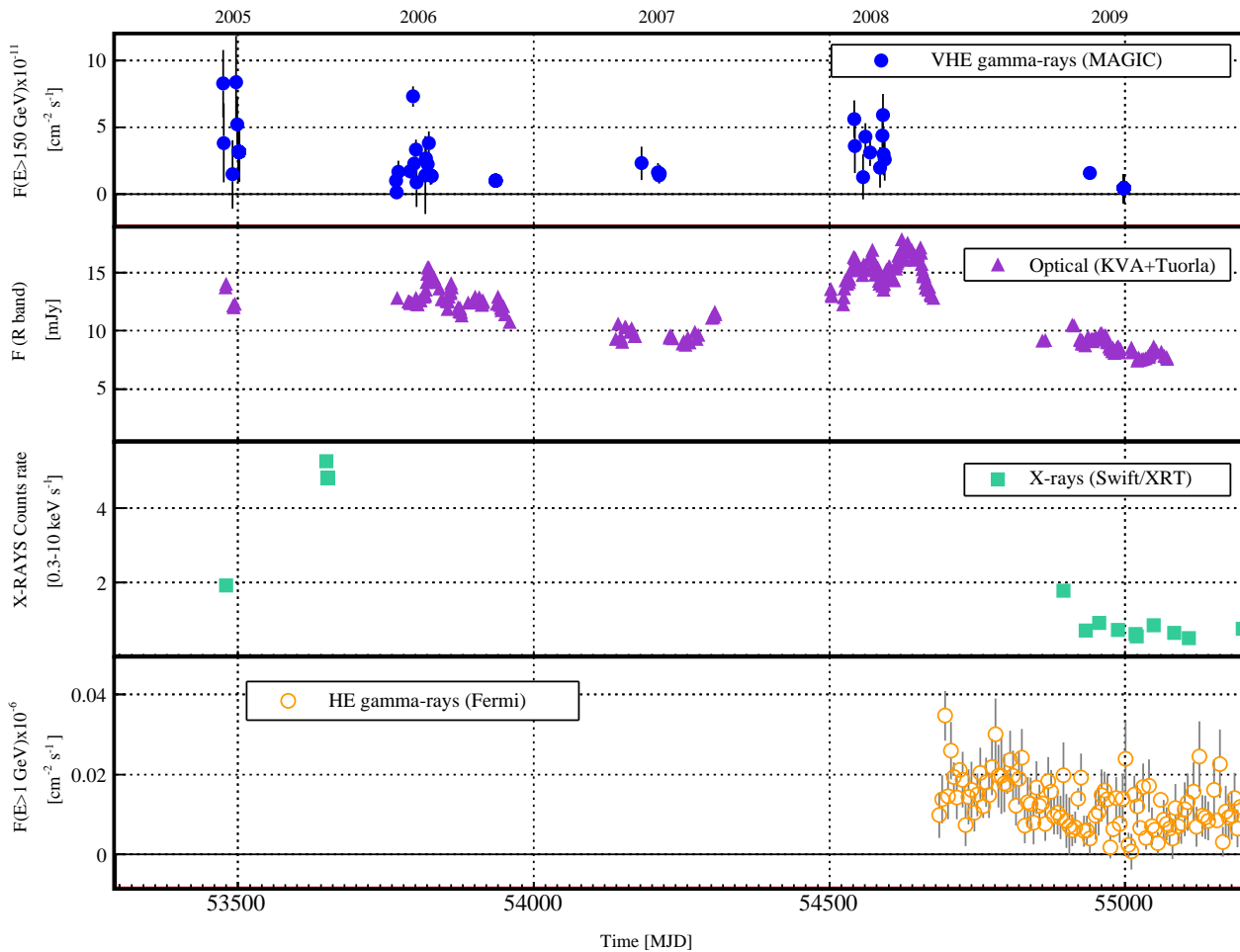


FIG. 1.— Multiwavelength light curve of PG 1553+113 from 2005 to late 2009. From upper to lower panel: VHE γ -rays above 150 GeV measured by MAGIC (filled circles), optical flux in the R-band (triangles), X-rays counts rate (squares) and soft γ -rays above 1 GeV (open circles). The error bars reported have 1σ significance.

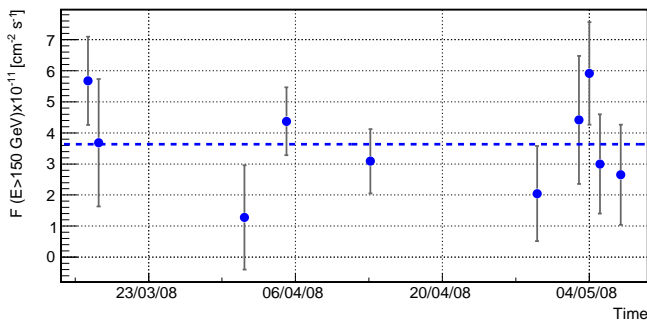


FIG. 2.— Zoom of Figure 1 around 2008 MAGIC observations.

In order to explore the VHE γ -ray emission of PG 1553+113 from each year, we compared the integral flux above 150 GeV. This value is a safe compromise taking into account the different energy thresholds. The final samples and the results of the spectral analyses are shown in Table 3.

The integral fluxes measured above 150 GeV lie in the range of 4% to 11% of the Crab Nebula flux measured by MAGIC (Albert et al. 2008a): the highest flux level is recorded in 2008 (0.11 Crab units), a factor between two to three larger compared to the one measured in 2007 (0.04 Crab units) and 2009 (0.05 Crab units).

Such changes in the flux level observed in PG 1553+113 are quite moderate in comparison to other monitored TeV blazars. For example, in Mkn 421 a flux variation exceeding one order of magnitude have been observed (e.g. Fossati et al 2008).

A detailed study about possible flux level variations on short timescale was carried out with the limiting condition that the signal is not strong enough to allow for a detailed sampling on sub-day timescale. The upper panel of Figure 1 displays the light curve of PG 1553+113 measured from 2007 to 2009 by MAGIC with a variable binning. For comparison, the daily flux levels measured in 2005 and 2006 are shown, as extrapolated from the published data (Albert et al. 2007a), and rescaled according to the power laws that interpolate the differential fluxes. Furthermore, the 2006 mean integral flux above 150 GeV taken during the multiwavelength campaign and reported in Albert et al. (2009) is shown. The former data have not been used for the integral flux study, due to very large uncertainties related to the extrapolation procedure. We set 2-days, daily and monthly binning for the 2007, 2008 and 2009 data sets respectively, according to the significance of the signal. We found a hint of variability within a factor of 4 during the period monitored in 2008. However, a constant fit to 2008 data drawn in Figure 2 has a probability of 50%.

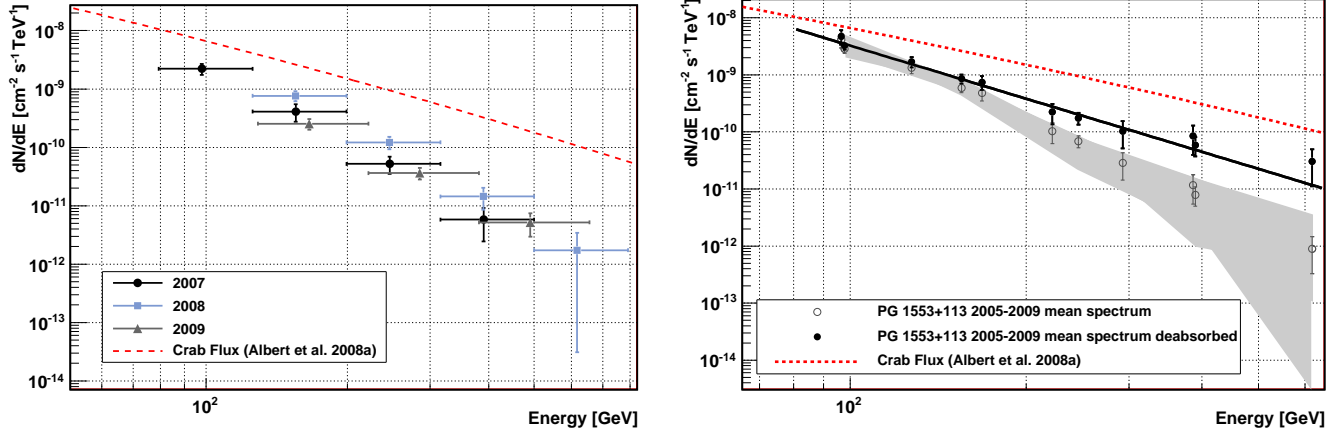


FIG. 3.— Differential energy spectra from PG 1553+113. Left Figure: comparison between 2007, 2008 and 2009 spectra. Right Figure: superimposition of 2005-2006 spectrum, from Albert et al. (2007a), to 2007-2009 mean spectrum and corresponding deabsorption for $z = 0.4$ using the EBL model of Dominguez et al. (2010). In both figures, the fit of the Crab Nebula spectrum measured by MAGIC (Albert et al. 2008a) is superimposed for comparison.

TABLE 3
PG 1553+113 MEASURED SPECTRA

Year	time [h]	$F > 150 \text{ GeV}$ [$10^{-11} \text{ cm}^{-2} \text{ s}^{-1}$]	$F > 150 \text{ GeV}$ [Crab %]	Γ
2007	11.5 h	1.40 ± 0.38	4%	4.1 ± 0.3
2008	8.7 h	3.70 ± 0.47	11%	4.3 ± 0.3
2009	6.9 h	1.63 ± 0.45	5%	3.6 ± 0.5

^aSpectra of the individual years of observations of PG 1553+113. From left to right: Year of MAGIC observations; Effective time in hours; Integral flux above 150 GeV in units of $10^{-11} \text{ cm}^{-2} \text{ s}^{-1}$ and Crab Nebula %; in the last column, the Γ indices obtained by fitting the observed differential spectra with a power law.

In 2007, the flux values, resulting from the temporal analysis, are in good agreement with the hypothesis of constant flux (93% of probability). Nothing can be concluded about 2009, since the significance of the signal is too low and prevents a detailed temporal study.

In general, the high energy threshold of the analysis together with the weakness of the PG 1553+113 signal and its very steep spectrum make any variability study at small timescale difficult and might have hid the detection of an increased activity on very short timescale. In order to detect or exclude TeV flares from this source, a more sensitive instrument should be used. For this purpose, PG 1553+113 is regularly monitored by the upgraded MAGIC stereo system.

3.2. Differential Flux

The differential spectra observed from PG 1553+113 by MAGIC every year from 2007 to 2009 are shown in the left plot of Figure 3.

As for other blazars, each spectrum can be well fitted with a power law function of the form

$$\frac{dF}{dE} = f_0 * \left(\frac{E}{200 \text{ GeV}} \right)^{-\Gamma} \quad (1)$$

where f_0 is the flux at 200 GeV and Γ is the power law index. The resulting indices are listed in the last column of Table 3. The systematic uncertainty is estimated to be 35% in the flux level and 0.2 in the power index (Albert et al. 2008a), and is the sum of many contributions, mainly due to the use of MC simulation instead of

test beams. Thanks to the low energy threshold of the analysis of 2007 data, the corresponding spectrum has a measured point below 100 GeV. This point is, within the errors, in good agreement with the low energy point measured in 2005 and 2006. The 2008 differential spectrum is in good agreement with the spectrum determined during a multiwavelength campaign with other instruments (Aleksić et al. 2010). Finally, the 2009 differential spectrum is scarcely determined due to the limited signal. Except for the latter sample, whose significance is rather low and corresponding errors noticeably large, the power law indices describing the spectra are compatible. This indicates that the shape of the emitted spectrum does not change, even if the total flux shows hints of (small amplitude) variability, as also noted for other BL Lacs such as 1ES 1218+304 (Acciari et al. 2010).

The right plot of Figure 3 shows the combined differential spectrum of PG 1553+113 from 2007 to 2009, superimposed to the 2005-2006 spectrum measured by MAGIC ($\Gamma = 4.21 \pm 0.25$, Albert et al. 2007a). The gray band represents the systematic effect on the combined spectrum result of different unfolding methods. The good agreement among these mean determinations suggests that despite the (small) variability seen on yearly scale, the mean flux emitted by this source is stable. A power law fit gives the values $\Gamma = 4.27 \pm 0.14$ for the index and $f_0 = (1.61 \pm 0.14) \cdot 10^{-10} \text{ s}^{-1} \text{ cm}^{-2} \text{ TeV}^{-1}$ for the normalization factor, with a $\chi^2/\text{dof} = 5.68/9$ and corresponding probability of 77%. The integral flux above 150 GeV is at the level of 8% of the Crab Nebula flux.

VHE photons from cosmological distances are absorbed in the interaction with the EBL. Taking into account the EBL absorption (Dominguez et al. 2010), the intrinsic spectrum is compatible with a power law of index 3.09 ± 0.20 , if we assume $z = 0.40$, as drawn in Figure 3.

4. PG 1553+113 AS SEEN AT OTHER WAVELENGTHS

Figure 1 displays the light curve of PG 1553+113 in different wavelengths. The MAGIC data shown cover five cycles of TeV observations at energies above 150 GeV. The time bins used are variable, as described in the pre-

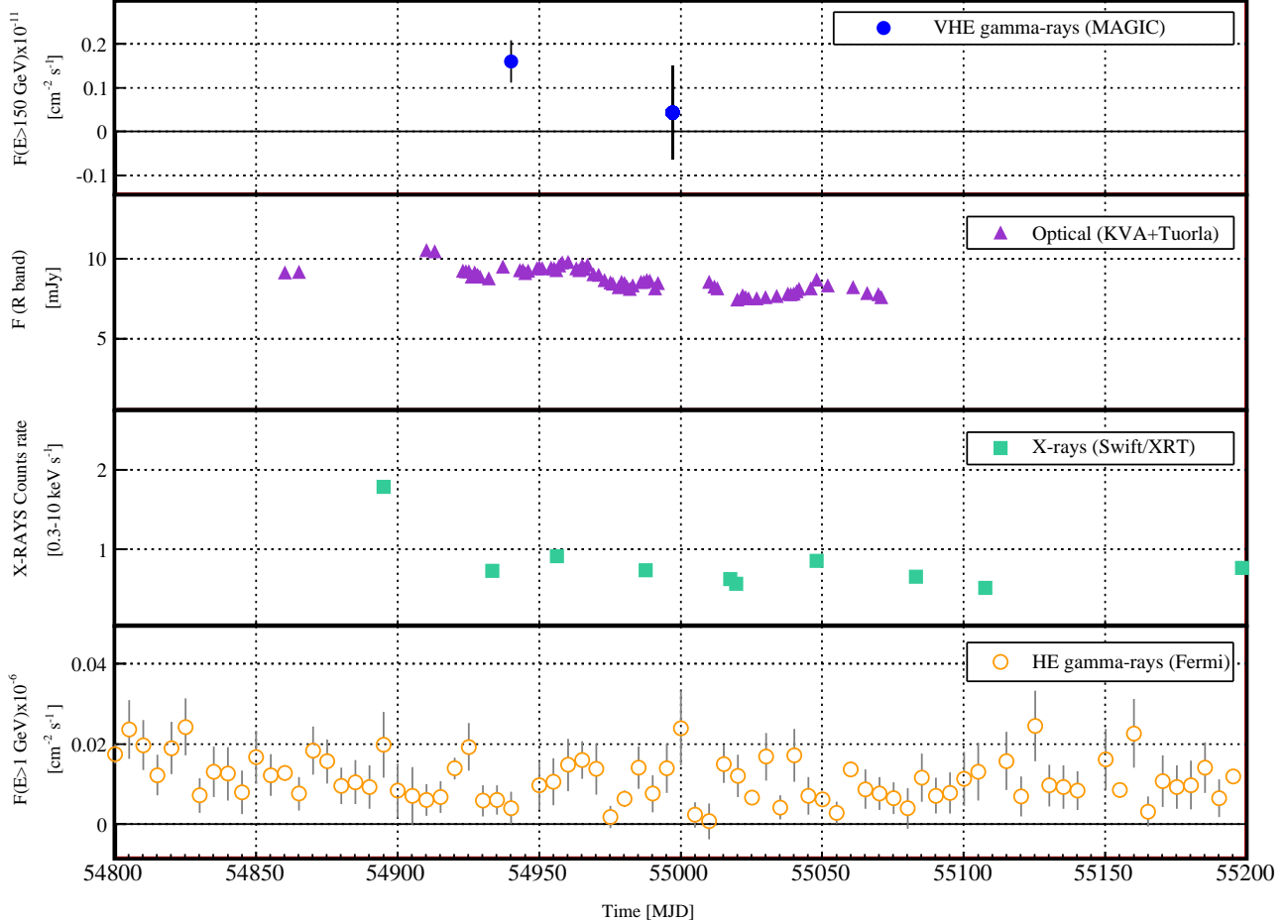


FIG. 4.— Zoom of Figure 1 around the Cycle V observations carried out in 2009. From upper to lower panel: VHE γ -rays above 150 GeV measured by MAGIC (filled circles), optical flux in the R-band (triangles), X-rays counts rate (squares) and soft γ -rays above 1 GeV (open circles).

vious Section.

The simultaneous optical R-band data are outlined in the second panel. These data are collected on a nightly basis by the Tuorla Observatory Blazar Monitoring Program¹ (Takalo et al. 2007) using the KVA 35 cm telescope at La Palma and the Tuorla 1 meter telescope in Finland. The public X-ray data, results of an automatic analysis performed by the Swift/XRT Monitoring Program², are shown in the third panel.

In the lower panel, the *Fermi*/LAT light curve of PG 1553+113 above 1 GeV, computed in bins of 5 days, is displayed. The light curve has been derived from the publicly available data³, which were processed using Science Tools 9.15.2, including the Galactic diffuse and isotropic background and the Instrument Response Function IRF P6 V3 DIFFUSE. We selected the photons of class 3 (DIFFUSE) with energy in the range 1–100 GeV collected between the beginning of Fermi data acquisition on 2008 August the 4th (MJD 54682) and 2010 January the 4th (MJD 55200), for a total of ~ 17 months of elapsed time. In each 5-days time bin, we selected photons in the good-time intervals and within a region

of interest (ROI) with radius of 10° from the position of the source in the radio band, applying a cut on the zenith angle parameter ($< 105^\circ$) to avoid the Earth’s albedo. Then we calculated the live-time, the exposure map and the diffuse response.

Taking all this into account, we performed an analysis of the high energy emission in each separate time bin, by using an unbinned likelihood algorithm (*gtlike*, Abdo et al. 2009b). The model included the isotropic and Galactic diffuse backgrounds, the source of interest, and all the 1FGL known γ -ray sources located within the ROI. For all point sources, we assumed a power law spectrum, with flux and photon index as a free parameter and calculated the corresponding test statistic (TS , see Mattox et al. 1996 for a definition; in practice one assumes $\sqrt{TS} \simeq \sigma$, the significance of the detection).

As already noted, during the five years of monitoring the source generally showed a marginal activity in the VHE γ -ray band. The same behavior is followed by the optical flux, whose variations are limited within a factor of four, with a maximum flux reached in 2008 and a minimum value in 2009. A low emission in 2009 is also registered at all the other wavelengths, (Figure 4), suggesting that the source entered in a low activity state during that year, with a minimum reached few days after MAGIC observations.

¹ More information at <http://users.utu.fi/kani/1m/>

² <http://www.swift.psu.edu/monitoring/>

³ Accessible from <http://fermi.gsfc.nasa.gov>

Figure 5 shows the result of a correlation study between optical and TeV simultaneous observations. The VHE γ -ray flux above 150 GeV is plotted as a function of the optical flux. In order to increase statistics, we used for 2007/8/9 samples the daily light curve values; however, since the optical measurements have a different time coverage, in some cases we estimated the mean VHE flux from two or more consecutive days. 2005 and 2006 data, from Albert et al. (2007a), were rejected from this study, due to the large uncertainty on the extrapolated flux in the VHE band. The mean flux value from 2006 multi-wavelength campaign, reported in Albert et al. (2009), is included. A linear relation among the two components has 76% of probability, which suggests a correlation between these two extreme energetic bands. This result is in good agreement with the SSC model, which predicts a correlation between the synchrotron and the IC emission, related to the same electron population. Due to the poor coverage at other wavelengths, the same study has not been performed in X rays and soft γ -rays.

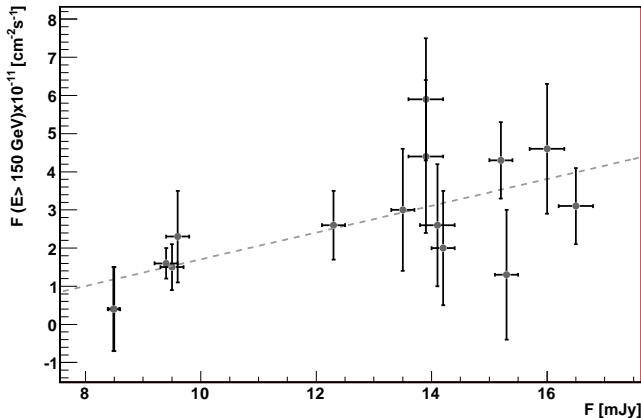


FIG. 5.— Correlation study between PG 1553+113 optical R-band flux and VHE γ -ray integral flux above 150 GeV observed from 2006 to 2009.

The X-ray light curve shows a pronounced variability, in contrast to optical and very high energy bands. The X-ray flux spans an interval of about one order of magnitude (with maximum in 2005 and minimum in 2009), larger than that observed in the TeV, optical and GeV bands. The different variability displayed by the synchrotron (X-ray) and inverse Compton (GeV-TeV) components seems to be somewhat in contrast with the typical behavior observed in TeV BL Lacs, showing, in general, a coordinated variability (e.g. Fossati et al 2008)⁴. However, the sparse sampling of the observations and the lack of a truly simultaneous monitoring prevents any strong conclusion. Coordinated multi-frequency monitoring is necessary to further investigate this important issue.

In a dedicated paper (Abdo et al. 2010b), the *Fermi*/LAT collaboration reported the analysis of the first year of PG 1553+113 data. They found that during the monitoring period the emission above 200 MeV is almost steady. This is in contrast with the behavior of

the source at larger energies (> 1 GeV). In our analysis of 2008 and 2009 LAT data drawn in lower panel of Figure 1, in fact, a steady emission above 1 GeV has a probability smaller than 0.1% and is ruled out. The lowest flux observed, in June 2009, is compatible with zero, while the highest flux, detected in August 2008, has a value $(0.035 \pm 0.006) \cdot 10^{-6} \text{ cm}^{-2} \text{ s}^{-1}$, a factor 3 higher with respect to the mean flux, $(0.0106 \pm 0.0004) \cdot 10^{-6} \text{ cm}^{-2} \text{ s}^{-1}$. In our case, we are looking only at the upper edge of LAT band, probably close to the IC peak, while the integral flux above 200 MeV reported by Abdo et al. (2010b) is dominated by lower energies, due to larger statistics. Therefore, we conclude that while at low energies the IC continuum shows marginal variability, this is not the case in the vicinity of the peak. In fact, small variability at GeV energies is a common feature of HBLs (e.g. Abdo et al. 2010a).

5. MODELING THE SED

In Figure 6, we assembled the SED of PG 1553+113 using historical data and the MAGIC spectra described above. Open black squares displaying radio-optical data are from NED⁵. In the optical band, we also show (red diamonds) the KVA minimum and maximum flux measured in the period covered by MAGIC 2005-2009 observations together with optical-UV fluxes from UVOT/*Swift* (filled black triangles, from Tavecchio et al. 2010). For the X-ray data, two XRT/*Swift* spectra taken in 2005 (high flux state, red crosses, and intermediate state, black asterisks, from Tavecchio et al. 2010) are given, and a *Suzaku* spectrum taken in 2006 (continuous red line, from Reimer et al. 2008). In addition, the average 14-150 keV flux measured by BAT/*Swift* during the first 39 months of survey (Cusumano et al. 2010) is shown (black star), and the average *RXTE*/ASM flux between March 1 and May 31, 2008 (small black square), from quick-look results provided by the ASM/*RXTE* team⁶.

The green triangles correspond to the LAT spectrum averaged over ~ 200 days (2008 August-2009 February) from Abdo et al. (2010b). As discussed in that paper, the flux above 200 MeV is rather stable, showing very small variability over the entire period of LAT observations. However, it is possible that variability at the highest energies is not detected due to the limited statistics, but is important in determining the averaged spectrum at the highest energies, as suggested in the previous Section.

For MAGIC, we report the 2005-2006 and 2007-2009 observed spectra (filled circles) and the same spectra corrected for the absorption by the EBL using the model of Dominguez et al. (2010) (red open circles).

We model the SED with the one-zone SSC model fully described in Maraschi & Tavecchio (2003). The emission zone is supposed to be spherical with radius R , in motion with bulk Lorentz factor Γ at an angle θ with respect to the line of sight. Special relativistic effects are described by the relativistic Doppler factor, $\delta = [\Gamma(1 - \beta \cos \theta)]^{-1}$. The electron energy distribution of the relativistic emitting electrons is described by a smoothed broken power law function, with limits γ_{\min} and γ_{\max} and break at γ_b .

⁴ Rare exceptions to this rule are the so called “orphan” TeV flares, e.g. Krawczynski et al. (2004)

⁵ <http://nedwww.ipac.caltech.edu/>

⁶ <http://xte.mit.edu/asmlc/>

To calculate the SSC emission, we use the full Klein–Nishina cross section.

Given the large variations of the X-ray synchrotron flux, we decided to use the average level of the synchrotron bump as measured by XRT, including also ASM and BAT fluxes to constrain the model. The corresponding input parameters are listed in Table 4. We also report the derived powers carried by the different components, relativistic electrons, P_e , magnetic field, P_B , and protons, P_p , (assuming a composition of one cold proton per relativistic electron) and the total radiative luminosity $L_r \simeq L_{\text{obs}}/\delta^2$.

TABLE 4
INPUT MODEL PARAMETERS FOR THE MODEL SHOWN IN FIG. 6

Parameter		Value
γ_{min}	$[10^3]$	2.5
γ_b	$[10^4]$	3.2
γ_{max}	$[10^5]$	2.2
n_1		2.0
n_2		4.0
B	[G]	0.5
K	$[10^3 \text{ cm}^{-3}]$	5.35
R	$[10^{16} \text{ cm}]$	1
δ		35
P_e	$[10^{44} \text{ erg/s}]$	2.2
P_B	$[10^{44} \text{ erg/s}]$	1.5
P_p	$[10^{44} \text{ erg/s}]$	0.34
L_r	$[10^{44} \text{ erg/s}]$	6.3

NOTE. — We list the minimum, break and maximum Lorentz factors and the low and high energy slope of the electron energy distribution, the magnetic field intensity, the electron density, the radius of the emitting region and its Doppler factor. We also give the derived power carried by electrons, magnetic field, protons (assuming one cold proton per emitting relativistic electron) and the total radiative luminosity.

The derived value of the total jet power, $P_{\text{jet}} = P_e + P_B + P_p = 4 \times 10^{44} \text{ erg/s}$, is consistent with the typical values inferred modelling similar sources (e.g. Ghisellini et al. 2010). We use a relatively large minimum electron Lorentz factor $\gamma_{\text{min}} \sim 10^3$ in order to reproduce the hard MeV–GeV continuum tracked by LAT. The high value of γ_{min} implies that, as commonly derived in TeV BL Lacs, the relativistic electrons (and the magnetic field, almost in equipartition) carry more power than the cold proton component. Another characteristics that PG 1553+113 shares with the other TeV BL Lacs is that the total luminosity L_r is larger than the power supplied by electrons, magnetic field and protons. As discussed in Celotti & Ghisellini (2008), this implies that either only a small fraction of leptons is accelerated at relativistic energies (leaving a reservoir of cold pairs and/or protons) or that the jet is dissipating a large fraction of its power as radiation, eventually leading to the deceleration of the flow, as in fact observed at VLBI scales (Piner et al. 2010) and envisaged in the models of structured jets (Georganopoulos & Kazanas 2003; Ghisellini et al. 2005).

6. CONCLUSIONS

In this paper, we presented the analysis of three years of VHE γ -ray data of PG 1553+113 collected by MAGIC

from 2007 to 2009. The data set was divided into individual years, and a significant signal was found in every sample, confirming PG 1553+113 as a stable presence in the VHE sky. The overall flux above 150 GeV from 2007 to 2009 shows only a modest variability on yearly time-scale, within a factor 3, corresponding to a variation between 4% to 11% of the Crab Nebula flux. No clear variability on smaller time-scale is evident in the sample.

For the spectral analysis, the data set was combined with previous observations carried out by MAGIC during the first two Cycles of operations, from 2005 to 2006, for a total of five years of monitoring. This sample was excluded from the temporal study due to very large systematics related to the flux extrapolation procedure. Despite the hints of variability on the flux level, the differential flux from each year is in very good agreement with a power law of constant index 4.27 ± 0.14 . This behavior has been already observed in other blazars, such as the HBL 1ES 1218+304 (Acciari et al. 2010).

PG 1553+113 was also monitored in optical, X-ray and soft γ -ray frequencies, but only the former data could be used for correlation studies thanks to the good time coverage. Interestingly, a hint of correlation with probability of 76% was found between MAGIC and R-band optical flux levels, which in turn shows only a modest variability within a factor 4. A clear variability is seen in X-rays and γ -rays above 1 GeV. The latter outcome, exploring the energies close to the IC peak, is only apparently in contradiction with previous results stating a quite stable spectrum for this source in the soft ($> 200 \text{ MeV}$) γ -ray band (Abdo et al. 2010b). The different energy thresholds used in the two studies can, in fact, explain very well the discrepancy, as discussed in the paper.

Finally, for the study of the spectral energy distribution, the mean differential spectrum measured by MAGIC was combined with historical data at other wavelengths. Due to the large variations observed in X-rays and characterizing the synchrotron peak, we decided to use for the SED modeling the high energy bump, and the average level of the low energy bump. A more precise model requires coupling the VHE γ -ray part of the spectrum with simultaneous coverage of the synchrotron peak, in particular at optical–X-ray energies. An interesting feature of PG 1553+113 is the narrowness of the SSC peak derived from the LAT and MAGIC spectra, implying a relatively large value of the minimum Lorentz factor of the emitting electrons, 2.5×10^3 . This is also required by other HBLs with hard GeV spectra (e.g. Tavecchio et al. 2010).

The MAGIC stereo system, with its increased sensitivity and low energy threshold, is the suitable instrument to further investigate eventual daily scale TeV variability, as well as provide a good differential spectrum determination below 100 GeV.

ACKNOWLEDGEMENTS

We would like to thank the Instituto de Astrofísica de Canarias for the excellent working conditions at the Observatorio del Roque de los Muchachos in La Palma. The support of the German BMBF and MPG, the Italian INFN, the Swiss National Fund SNF, and the Spanish MICINN is gratefully acknowledged. This work was also supported by the Marie Curie program, by the CPAN

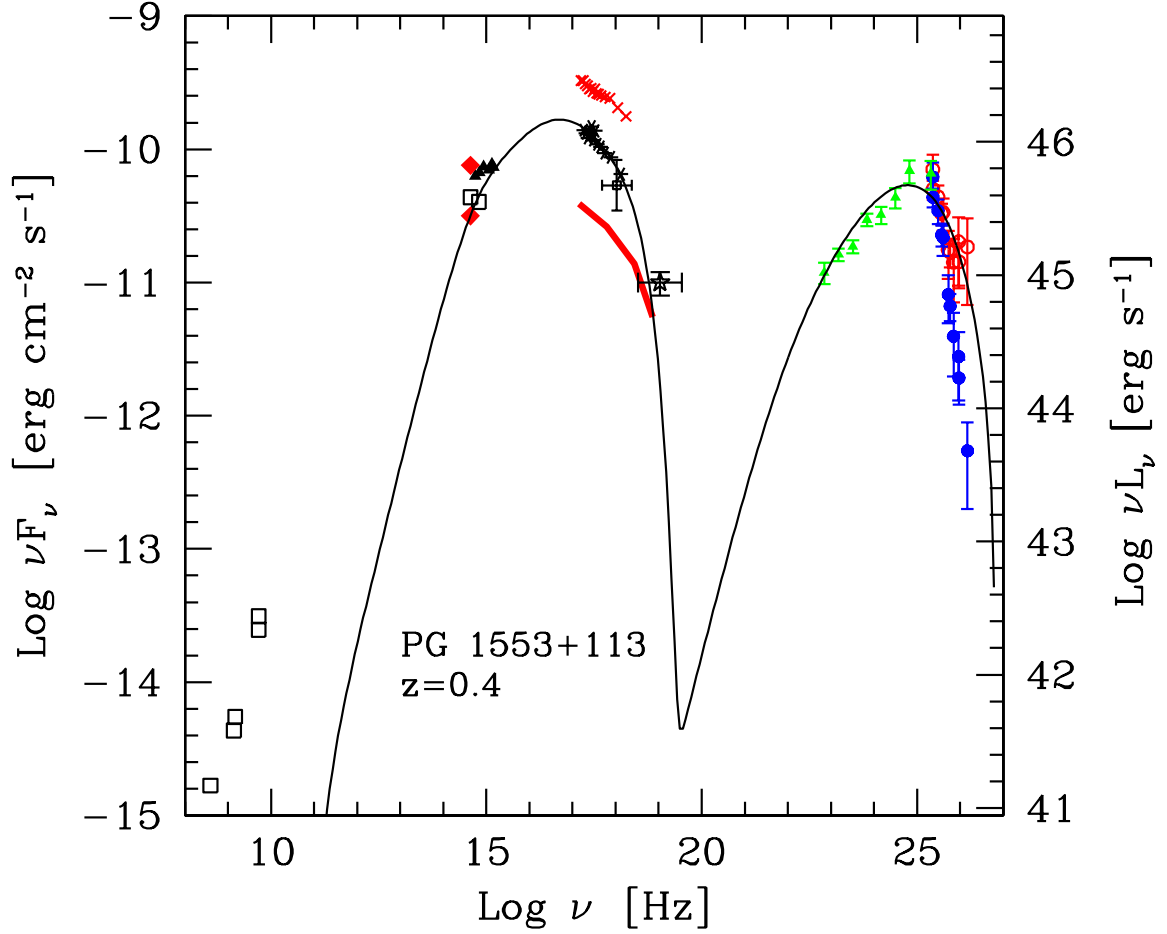


FIG. 6.— SED of PG 1553+113. Open black squares are radio-optical data from NED, red diamonds represent the KVA minimum and maximum flux measured in the period covered by MAGIC observations, together with optical-UV fluxes from UVOT/*Swift* (filled black triangles). For the X-ray data, two XRT/*Swift* spectra taken in 2005 (high flux state, red crosses, and intermediate state, black asterisks) are given, and a *Suzaku* spectrum taken in 2006 (continuous red line). The average 14-150 keV flux measured by BAT/*Swift* (black star) and the average *RXTE*/ASM flux between March 1 and May 31, 2008 (small black square), are also represented. The LAT spectrum averaged over ~ 200 days (2008 August-2009 February) is given (green filled triangles). For MAGIC, we display the 2005-2006 and 2007-2009 observed spectra (blue filled circles) and the same spectra corrected for the absorption by the EBL (red open circles). The SED is modeled with a one-zone SSC model (continuous black line). Detailed references are addressed in the text.

CSD2007-00042 and MultiDark CSD2009-00064 projects of the Spanish Consolider-Ingenio 2010 programme, by grant DO02-353 of the Bulgarian NSF, by grant 127740

of the Academy of Finland, by the YIP of the Helmholtz Gemeinschaft, by the DFG Cluster of Excellence “Origin and Structure of the Universe”, and by the Polish MNiSzW Grant N N203 390834.

REFERENCES

- Abdo, A. A., et al. 2010a, *ApJ*, 722, 520
 Abdo, A. A., et al. 2010b, *ApJ*, 708, 1310
 Abdo, A. A., et al. 2009a, *ApJ*, 700, 597
 Abdo, A. A., et al. 2009b, *ApJS*, 183, 46
 Acciari, V. A., et al. 2010, *ApJ*, 709, L163
 Aharonian, F., et al. 2006a, *A&A*, 448, L19
 Aharonian, F., et al. 2006b, *Nature* 440, 1018
 Albert, J. et al. 2009, *A&A* 493, 467
 Albert, J., et al. 2008a, *ApJ*, 674, 1037
 Albert, J., et al. 2008b, *ApJ*, 685, L23
 Albert, J., et al. 2008c, *Nucl. Instr. Meth. A* 588, 424
 Albert, J., et al. 2007a, *ApJ Letters*, 654, L119
 Albert, J., et al., 2007b, *Nucl. Instr. Meth. A* 583, 494
 Aleksić, J., et al. 2010, *A&A* 515, A76
 Aliu, E., et al. 2009, *ApJ*, 30, 293
 Baixeras, C., et al. 2004, *Nucl. Instrum. Meth. A* 518, 188
 Britzger, D., Carmona, E., Majumdar, P., Blanch, O., Rico, J., Sitarek, J., & Wagner, R. 2009, in *Proc. 31st Int. Cosmic Ray Conf.*, preprint (arXiv:0907.0973)
 Celotti, A., & Ghisellini, G. 2008, *MNRAS*, 385, 283
 Cortina, J., Goebel, F., & Schweizer, T. 2009, preprint arXiv:0907.1211
 Cusumano, G., et al. 2010, *A&A*, in press
 Danforth, C. W., Keeney, A. B., Stocke, J. T., Michael Shull, J., & Yao, J. 2010, *ApJ*, 720, 976
 Dominguez, A., et al. 2010, *MNRAS*, accepted

- Fomin, V. P., et al. 1994, *ApJ*, 2, 137
Fossati, G., et al. 2008, *ApJ*, 677, 906
Georganopoulos, M., & Kazanas, D. 2003, *ApJ*, 594, L27
Ghisellini, G., et al. 2010, *MNRAS*, in press
Ghisellini, G., Tavecchio, F., & Chiaberge, M. 2005, *A&A* 432, 401
Green, R. F., Schmidt, M., & Liebert, J. 1986, *ApJS*, 61, 305
Krawczynski, H., et al. 2004, *ApJ*, 601, 151, 2004
Mannheim, K. 1993, *A&A*, 269, 67
Mattox, J. R., et al., 1996, *ApJ*, 461, 396
Mazin, D., & Goebel, F. 2007, *ApJ Letters* 655, L13
Maraschi, L., & Tavecchio, F. 2003, *ApJ*, 593, 667-675
Li, T. P., & Ma, Y. Q. 1983, *ApJ*, 272, 317
Piner, B. G., Pant, N., & Edwards, P. G. 2010
Prandini, E., Bonnoli, G., Maraschi, L., Mariotti, M., & Tavecchio, F. 2010, *MNRAS* 405, L76
Reimer, A., Costamante, L., Madejski, G., Reimer, O., & Dorner, D. 2008, *ApJ*, 682, 775
Sbarufatti, B., Treves, A., & Falomo, R. 2005, *ApJ*, 635, 173
Stecker, F. W., de Jager, O. C. & Salamon, M.H. 1992, *ApJ* 390, L49
Takalo, L. O., et al. 2007, *ASP Series*, 373, 249
Tavecchio, F., Ghisellini, G., Ghirlanda, G., Foschini, L., & Maraschi, L. 2010, *MNRAS*, 401, 1570
Treves, A., Falomo, R., & Uslenghi, M. 2007, *A&A*, 473, L17
Urry, C. M., & Padovani, P. 1995, *PASP*, 107, 803